

# A Molecular Platinum Cluster Junction: A Single-Molecule Switch

Linda A. Zotti,<sup>\*,†</sup> Edmund Leary,<sup>†,‡</sup> Maria Soriano,<sup>†,§</sup> Juan Carlos Cuevas,<sup>||</sup> and Juan Jose Palacios<sup>†</sup>

<sup>†</sup>Departamento de Física de la Materia Condensada, Universidad Autónoma de Madrid, 28049 Madrid, Spain

<sup>‡</sup>Instituto Madrileño Estudios Avanzados (IMDEA) Nanociencia, E-28049 Madrid, Spain

<sup>§</sup>Departamento de Física Aplicada, Universidad de Alicante, 03690 Alicante, Spain

<sup>||</sup>Departamento de Física Teórica de la Materia Condensada, Universidad Autónoma de Madrid, E-28049 Madrid, Spain

## Supporting Information

**ABSTRACT:** We present a theoretical study of electron transport through single-molecule junctions incorporating a Pt<sub>6</sub> metal cluster bound within an organic framework. The insertion of this molecule between a pair of electrodes leads to a fully atomically engineered nanometallic device with high conductance at the Fermi level and two sequential high on/off switching states. The origin of this property can be traced back to the existence of a degenerate HOMO consisting of two asymmetric orbitals with energies close to the Fermi level of the metal leads. The degeneracy is broken when the molecule is contacted to the leads, giving rise to two resonances that become pinned to the Fermi level and display destructive interference.

Molecular metal clusters (MCs) have recently been explored in break-junction-type single-molecule (SM) conductance experiments,<sup>1–3</sup> while previous studies investigated clusters using scanning tunneling microscopy/spectroscopy (STM/STS), which maintains a tunneling gap between the tip and the molecule.<sup>4,5</sup> MCs have fewer metal atoms but more precisely defined composition and structure than metal nanoparticles and thus are better suited for comparative studies between theory and experiment. Bare MCs have been successfully deposited and studied on various surfaces<sup>6</sup> but require very clean conditions for study because of their high reactivity. To overcome this difficulty and enable the study of MCs under the normal ambient conditions of the break-junction experiment, the metal atoms must be encapsulated in a ligand sphere to avoid unwanted chemical reactions with the atmosphere. Ligand-stabilized MCs, particularly those incorporated in organic frameworks (OFs), have been suggested as components of data storage devices, where they would act as nanocapacitors because of their redox properties.<sup>7</sup> Transport measurements on individual MCs are still rare, however. Metal atoms and chains of atoms have been successfully incorporated into OFs as metal complexes for SM experiments.<sup>8</sup> The Mn<sub>12</sub> structure has been investigated as the functional core in SM magnets,<sup>1</sup> and its transport properties have been studied theoretically.<sup>9,10</sup> However, despite the vast range of known MCs, only a few have been analyzed in this context. This is especially true regarding the theory of electron transport.<sup>11,12</sup>

In ref 2, SM experiments on [Pt<sub>6</sub>(μ-P<sup>t</sup>Bu<sub>2</sub>)<sub>4</sub>(CO)<sub>4</sub>(S(CH<sub>2</sub>)<sub>4</sub>SH)<sub>2</sub>]<sub>3</sub>, hereafter denoted as (SC<sub>4</sub>S)<sub>2</sub>Pt<sub>6</sub>, were carried

out using the STM-based *I*(*s*) technique.<sup>13</sup> The structure of (SC<sub>4</sub>S)<sub>2</sub>Pt<sub>6</sub> makes it ideal for these kind of measurements, as the butanedithiol (SC<sub>4</sub>S) chains are oriented trans to each other, producing a linear wire. Without these chains, it would be difficult to determine the precise points of attachment of the molecule to the electrodes. The presence of these groups not only provides robust thiol anchors but also increases the total length of the molecule in one defined direction, allowing measured break-off distances for accurate assessment of the orientation of the molecule in the junction (the need to incorporate the MC in a wire has also been suggested in a theoretical study of the electronic transport through a Mn<sub>12</sub> cluster<sup>10</sup>). In ref 2, it was suggested that the presence of the Pt cluster increases the conductance (*G*) compared with an alkane chain of equivalent length because Pt states exist in close proximity to the Fermi level. These were claimed to create an indentation in the potential barrier, giving a molecular analogue of an inorganic double tunneling barrier (DTB) in which the Pt<sub>6</sub> unit acts as a well and the SC<sub>4</sub>S chains act as barriers that decouple the central unit from the leads. This speculative argument was not fully proven, and the nature of these states was not identified. Assessing this assertion is important because the DTB configuration could be a basis for creating molecular switches<sup>14</sup> analogous to conventional electronic components, one of the main aims of molecular electronics.<sup>15</sup> Here we performed first-principles calculations to find out whether the assumptions made in the experimental work could be corroborated [details about our calculations and geometry constructions are reported in the Supporting Information (SI)]. We found that the highest occupied molecular orbital (HOMO) of (SC<sub>4</sub>S)<sub>2</sub>Pt<sub>6</sub> consists of two degenerate levels that become pinned to the Fermi level when the molecule is placed between two Au electrodes. However, these two levels do not originate simply from the Pt<sub>6</sub> unit but also contain states localized on the ligands. Moreover, interesting interference features appear in the transmission curve at the Fermi level.

We first studied the molecule in the gas phase. The optimized geometry consists of a Pt<sub>6</sub> cluster sandwiched between two SC<sub>4</sub>S chains (Figure 1). The central cluster consists of two orthogonal Pt<sub>3</sub> triangles, as confirmed by crystallographic analysis of the carbonyl-substituted compound.<sup>16</sup> Each Pt<sub>3</sub> triangle contains two bridging P<sup>t</sup>Bu<sub>2</sub> groups, and the remaining sides are joined together to form a tetrahedral Pt core, which also contains four

Received: October 16, 2012

Published: January 18, 2013

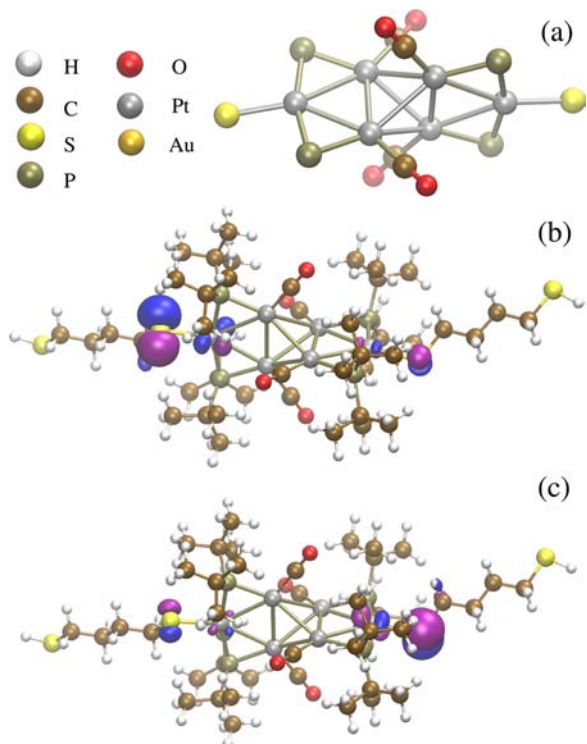


**Figure 1.** (a) Central moiety of  $(SC_4S)_2Pt_6$ . (b, c) Optimized geometry of  $(SC_4S)_2Pt_6$  showing the degenerate HOMO levels.

CO ligands. The molecule is slightly bent, with the angle between the alkyl chains less than  $180^\circ$ . The HOMO consists of two doubly occupied degenerate levels that are related to each other by an  $S_4$  rotation (Figure 1b,c). It is mainly localized on the two innermost S atoms and the two neighboring Pt atoms. These frontier molecular orbitals (FMOs) are different from the HOMO shown in ref 16 because of the presence of the  $SC_4S$  ligands. To show whether the presence of the Pt cluster provides a significant change in  $G$ , we also studied a  $C_{18}H_{36}$  alkyl chain terminated with S atoms (denoted as  $SC_{18}S$ ), as it was claimed to have the same length as  $(SC_4S)_2Pt_6$  but a much lower  $G$ .<sup>2</sup> The length of  $SC_{18}S$  was found to be 24.9 Å, which is halfway between the through-space S–S distance (23.9 Å) and the sum of the lengths of two  $SC_4S$  chains and the Pt core (25.8 Å) in  $(SC_4S)_2Pt_6$ . In  $SC_{18}S$ , the HOMO is localized on the S atoms, while the HOMO–1 is delocalized over the whole chain.<sup>15</sup> It should be noted that both molecules terminate with H atoms in the gas phase.

We next studied  $(SC_4S)_2Pt_6$  and  $SC_{18}S$  junctions bound to the Au clusters in top and hollow geometries (Figure 2). Figure 3 shows the transmission curves for all four cases. For  $SC_{18}S$ , the energy alignment is considerably affected by the binding geometry. The energy of HOMO–1 (which is delocalized over the whole chain and gives the main contribution to the transmission<sup>15</sup>) is lower in the hollow geometry than in the top geometry, yielding a 1 order of magnitude difference in  $G$  for the two geometries. Also, the presence of the HOMO (localized on the S atoms) very close to the Fermi level is clearly visible as a bump in the transmission curve for the top geometry. For  $(SC_4S)_2Pt_6$ , the alignment of the HOMOs does not show a particular dependence on the binding geometry, as they are pinned at the Fermi level in both cases, but their splitting is affected. The degeneracy of the HOMOs is broken in the junction, as the symmetry changes upon geometry relaxation. We

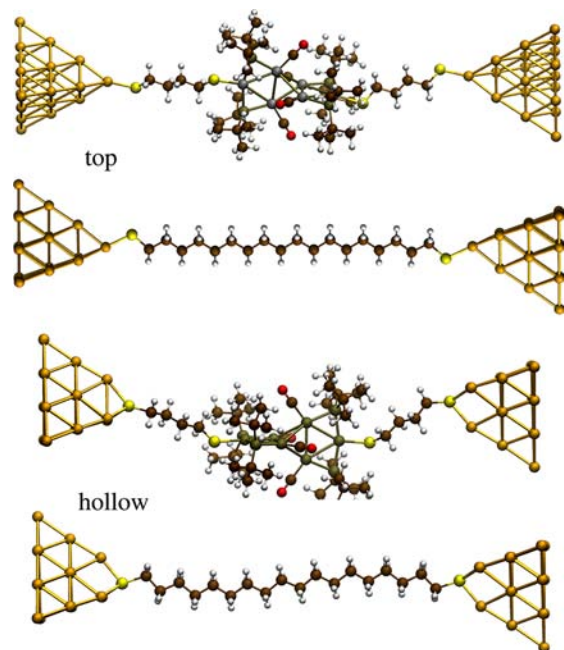


**Figure 2.** Optimized geometries of  $(SC_4S)_2Pt_6$  and  $SC_{18}S$  embedded between Au clusters.

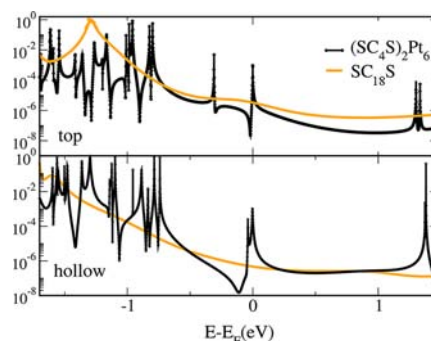


**Figure 3.** Transmission curves for the studied molecular junctions.

stress that the two peaks close to the Fermi level arise not simply from the  $Pt_6$  unit, as suggested in ref 2, but rather from orbitals containing contributions from both S and Pt atoms, as discussed above.

Fermi level pinning has been widely studied, but its nature is still under discussion (see ref 17 and references therein). It is also well-known that molecular HOMO–LUMO gaps are usually underestimated by DFT and that this affects the  $G$  values in DFT-based transmission calculations. To gain insight into the level alignment in our calculations and to understand whether it is reliable, we evaluated the ionization potential (IP) and electron affinity (EA) in the gas phase for the two molecules [calculated as  $E(N) - E(N - 1)$  and  $E(N + 1) - E(N)$ , respectively, where  $N$  is the total number of electrons]. These quantities (based on total energy differences) are expected to be more reliable than the HOMO and LUMO energies assigned by the Kohn–Sham states [–4.27 and –3.07 eV for  $(SC_4S)_2Pt_6$  and –5.3 and –0.08 eV for  $SC_{18}S$ , respectively]. The calculated IP and EA in the gas phase were found to be –5.66 and –1.70 eV for  $(SC_4S)_2Pt_6$  and –7.4 and 0.45 eV for  $SC_{18}S$ , respectively. Molecular HOMO–LUMO gaps are expected to narrow when molecules approach metal electrodes because of the screening effect.<sup>18</sup> Since the IP of  $(SC_4S)_2Pt_6$  is very close to the Fermi level of Au (–5.0 eV), it is

plausible that contacting the molecule to the electrode raises the IP to a point where it becomes pinned to the Fermi level. This is accompanied by charge transfer from the molecule to the metal, as confirmed by the positive charges of  $1.47e$  and  $4.3e$  found on the molecule in the top and hollow positions, respectively. The transferred charge originates mostly from the S atoms directly connected to the leads. On the basis of the proximity of the IP to the Au Fermi level, we believe that the energy alignment of the HOMO states appearing in our transmission curves for  $(SC_4S)_2Pt_6$  is robust and unaffected by common DFT failures, providing a realistic picture of the experimental scenario. In contrast, the calculated gas-phase IP of  $SC_{18}S$  is much lower than the peak corresponding to the HOMO (localized on the S atoms) in the transmission curve for the Au– $SC_{18}S$ –Au junction, especially for the top binding geometry. This suggests that it should align at lower energy; if so, the  $G$  values for  $SC_{18}S$  should be significantly lower than those we computed.

A further significant result is the presence of interference resonances in the transmission curves, which are clearly visible in Figure 3. The interest in interference effects in molecular junctions is steadily growing<sup>19</sup> because they modify the thermoelectric properties of the junctions,<sup>15</sup> and the ensuing dips in the transmission curves could give rise to large on/off ratios in future molecule-based electronic devices.<sup>19c</sup> Interference effects have recently been detected experimentally in molecular junctions.<sup>20</sup> Here they originate from the existence of two possible pathways (the two HOMO states). For the top position, we found a feature similar to that produced in ref 21. Interferences yielding peaks at the Fermi level have been predicted previously,<sup>22</sup> but to the best of our knowledge, their occurrence from two degenerate levels pinned at the Fermi level is rare. To shed light on the origin of these interference features, we built a simple model involving two levels connected to the leads (Figure 4). These levels are related to the two HOMO

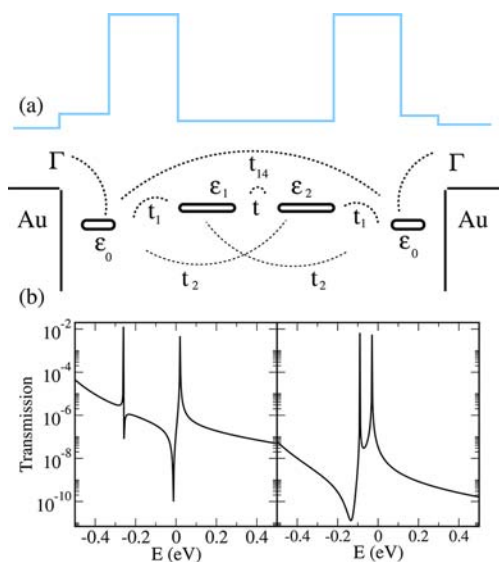


**Figure 4.** (a) Schematic representations of the model describing the interference effects close to the Fermi energy (black) and the double tunneling barrier (blue). (b) Corresponding transmission as a function of energy for (left) the top position with the parameter values  $\Gamma = 0.05$  eV,  $\epsilon_0 = -0.7$  eV,  $\epsilon_1 = \epsilon_2 = -0.12$  eV,  $t_1 = 0.009$  eV,  $t_2 = 0.005$  eV,  $t = 0.14$  eV, and  $t_{14} = 0.003$  eV and (right) the hollow geometry with the parameter values  $\Gamma = 0.05$  eV,  $\epsilon_0 = -0.7$  eV,  $\epsilon_1 = \epsilon_2 = -0.06$  eV,  $t_1 = 0.005$  eV,  $t_2 = 0.002$  eV,  $t = 0.03$  eV, and  $t_{14} = 0.000145$  eV.

levels of  $(SC_4S)_2Pt_6$ , which are degenerate and orthogonal in the gas phase. However, when the molecule is placed between two electrodes, the symmetry and consequently the degeneracy are broken because of the geometrical readjustment of the molecule. Thus, in our model (see the SI), the two states (with energies  $\epsilon_1$  and  $\epsilon_2$ ) are no longer eigenstates of the system and are coupled by a nonzero hopping matrix element,  $t$ . The interface levels (with energy  $\epsilon_0$ ) are coupled to the molecular states through  $t_1$  and  $t_2$  and to each other through  $t_{14}$ . The coupling  $t_1$  must be larger than  $t_2$  to account for the asymmetry of the orbitals. The couplings to the left and right leads ( $\Gamma_L$  and  $\Gamma_R$ , respectively) are in this case identical (i.e.,  $\Gamma_L = \Gamma_R = \Gamma$ ) because the junctions are symmetric.

As an example, Figure 4b shows the transmission curves given by this model for sets of parameters that reproduce the shapes of the DFT-calculated transmission curves for the hollow and top positions. This proves that the nature of the features appearing in the transmission curves at the Fermi level involves interference between the two levels of the central moiety and the two levels localized at the interfaces between this moiety and the leads. The transmission curve for an asymmetric junction (e.g., top–hollow) is expected to resemble that for the top–top case (see the SI).

As mentioned above, the presence of a resonance immediately followed by an antiresonance increases the on/off ratio in gating experiments. One can simply view this by imagining that the Fermi level (located at 0 eV) is shifted to more negative values along the energy axis. In the top geometry, for instance, the Fermi level would cross first a sharp peak (on) and then, after a very small shift, a sharp dip (off). This sequence would then be repeated as the Fermi level is shifted further and crosses the second resonance–antiresonance couple. Indeed, we propose that the low-bias conductance of this system should be measured as a function of the gate voltage to test the breaking of the degeneracy.

Finally, we compare our results with the experiments. In ref 2,  $G = 3 \times 10^{-5}G_0$  was measured for  $(SC_4S)_2Pt_6$ , while for  $SC_{18}S$ ,  $G$  was extrapolated to be  $6 \times 10^{-10}G_0$  using the experimental attenuation values measured for a series of shorter compounds. It was argued that the alkyl chains in  $(SC_4S)_2Pt_6$  act simply as spacers, as their FMOs lie far from the Fermi level, while the FMOs of the central unit create a barrier indentation and consequently raise  $G$  by  $\sim 6$  orders of magnitude relative to  $SC_{18}S$ . In our results, it is true that precisely at the Fermi level,  $G$  for  $(SC_4S)_2Pt_6$  is definitely higher than that for  $SC_{18}S$ ; however, at other energies immediately below or above it, the  $G$  value is comparable or even lower, especially as a result of the destructive interference. This could potentially explain nonlinearities observed in some of the experimental  $I$ – $V$  curves (see the SI for ref 2). It is also worth adding that because of the uncertainty about the precise length of  $(SC_4S)_2Pt_6$ , an exact comparison of the  $G$  values for  $(SC_4S)_2Pt_6$  and  $SC_{18}S$  is somehow ambiguous since in our equilibrium geometries  $SC_{18}S$  is straight (with only slight defects) whereas the cluster molecule is bent, with the  $Pt_6$  cluster slightly off the Au–Au axis. In the experiments, though,  $(SC_4S)_2Pt_6$  was probably straightened because of the pulling stress applied. Regardless of these uncertainties, the overall picture supports the naive idea based on the experimental findings, confirming the presence of resonances at the Fermi level arising from the presence of the additional central moiety in the molecular cluster.

In conclusion, we have theoretically studied SM junctions incorporating a  $Pt_6$  cluster and found that they act in a fashion



analogous to a double tunneling barrier due to two (originally degenerate) states that align at the Fermi level. These states do not stem from the Pt unit alone but specifically arise from two apical Pt atoms and their neighboring S atoms. This gives rise to quantum interference effects due to multiple electronic pathways through the molecule. Because of the Fermi level pinning, these effects should be easily detectable experimentally. Despite the seemingly apparent complexity of the structure, all of the physical properties arise from these four atoms alone, highlighting the delicate relationship between molecular structure and electrical properties. We propose that further chemical synthesis combined with theoretical calculations should be performed to explore other combinations of metal clusters with organic moieties. This could provide an alternate strategy for designing molecular devices that does not involve purely organic molecules because of the wealth of different structures possible via inorganic chemistry. Recent progress in implementing gates in SM-based devices<sup>23</sup> allows us to predict that the studied molecule, with its controlled binding to the electrodes and its two levels aligned at the Fermi level, could be used in a three-terminal device in which only a small gate voltage would be enough to pass through two high/low sequential switching states.

## ■ ASSOCIATED CONTENT

### ● Supporting Information

Details of the model shown in Figure 4, analysis of asymmetric junctions, and calculated Cartesian coordinates and total energies. This material is available free of charge via the Internet at <http://pubs.acs.org>.

## ■ AUTHOR INFORMATION

### Corresponding Author

[linda.zotti@uam.es](mailto:linda.zotti@uam.es)

### Notes

The authors declare no competing financial interest.

## ■ ACKNOWLEDGMENTS

This research was supported by the Comunidad de Madrid through Project NANOBIOIMAGNET S2009/MAT1726, the Generalitat Valenciana through Project PROMETEO2012/011, and the Spanish MICINN under Grants FIS2010-21883 and CONSOLIDER CSD2007-0010. E.L. was funded by the EU through the ELFOS Network (FP7-ICT2009-6). We thank the UAM CCC for computational resources.

## ■ REFERENCES

- (1) Heersche, H. B.; de Groot, Z.; Folk, J. A.; van der Zant, H. S. J.; Romeike, C.; Wegewijs, M. R.; Zobbi, L.; Barreca, D.; Tondello, E.; Corni, A. *Phys. Rev. Lett.* **2006**, *96*, No. 206801.
- (2) Leary, E.; van Zalinge, H.; Higgins, S. J.; Nichols, R. J.; de Biani, F.; Leoni, P.; Marchetti, L.; Zanello, P. *Phys. Chem. Chem. Phys.* **2009**, *11*, 5198.
- (3) Boardman, B. M.; Widawsky, J. R.; Park, Y. S.; Schenck, C. L.; Venkataraman, L.; Steigerwald, M. L.; Nuckolls, C. *J. Am. Chem. Soc.* **2011**, *133*, 8455.
- (4) Soldatov, E. S.; Gubin, S. P.; Maximov, I. A.; Khomutov, G. B.; Kolesov, V. V.; Sergeev-Cherenkov, A. N.; Shorokhov, V. V.; Sulaimankulov, K. S.; Suyatin, D. B. *Microelectron. Eng.* **2003**, *69*, 536.
- (5) Gubin, S. P.; Gulayev, Y. V.; Khomutov, G. B.; Kislov, V. V.; Kolesov, V. V.; Soldatov, E. S.; Sulaimankulov, K. S.; Trifonov, A. S. *Nanotechnology* **2002**, *13*, 185.
- (6) (a) Yasumatsu, H.; Hayakawa, T.; Kondow, T. *Chem. Phys. Lett.* **2010**, *487*, 279. (b) Isomura, N.; Wu, X.; Watanabe, Y. *J. Chem. Phys.* **2009**, *131*, No. 164707.

- (7) Femoni, C.; Iapalucci, M. C.; Kaswalder, F.; Longoni, G.; Zacchini, S. *Coord. Chem. Rev.* **2006**, *250*, 1580.
- (8) (a) Park, J.; Pasupathy, A. N.; Goldsmith, J. I.; Chang, C.; Yaish, Y.; Petta, J. R.; Rinkoski, M.; Sethna, J. P.; Abruna, H. D.; McEuen, P. L.; Ralph, D. C. *Nature* **2002**, *417*, 722. (b) Ruben, M.; Landa, A.; Lörtscher, E.; Riel, H.; Mayor, M.; Görls, H.; Weber, H. B.; Arnold, A.; Evers, F. *Small* **2008**, *4*, 2229. (c) Mayor, M.; von Hänisch, C.; Weber, H. B.; Reichert, J.; Beckmann, D. *Angew. Chem., Int. Ed.* **2002**, *41*, 1183. (d) Georgiev, V. P.; McGrady, J. E. *J. Am. Chem. Soc.* **2011**, *133*, 12590.
- (9) Renani, F. R.; Kirczenow, G. *Phys. Rev. B* **2011**, *84*, No. 180408.
- (10) Barraza-Lopez, S.; Park, K.; García-Suárez, V.; Ferrer, J. *J. Appl. Phys.* **2009**, *105*, No. 07E309.
- (11) Gerasimov, Y. S.; Shorokhov, V. V.; Soldatov, E. S.; Snigirev, O. V. *Proc. SPIE* **2010**, *7521*, 75210U.
- (12) Gerasimov, Y. S.; Shorokhov, V. V.; Maresov, A. G.; Soldatov, E. S.; Snigirev, O. V. *J. Commun. Technol. Electron.* **2011**, *56*, 1483.
- (13) (a) Haiss, W.; van Zalinge, H.; Higgins, S. J.; Bethell, D.; Höbenreich, H.; Schiffrin, D. J.; Nichols, R. J. *J. Am. Chem. Soc.* **2003**, *125*, 15294. (b) Nichols, R. J.; Haiss, W.; Higgins, S. J.; Leary, E.; Martin, S.; Bethell, D. *Phys. Chem. Chem. Phys.* **2010**, *12*, 2801.
- (14) Leary, E.; Higgins, S. J.; van Zalinge, H.; Haiss, W.; Nichols, R. J. *Chem. Commun.* **2007**, 3939.
- (15) Cuevas, J. C.; Scheer, E. *Molecular Electronics: An Introduction to Theory and Experiment*; World Scientific: Singapore, 2010.
- (16) de Biani, F. F.; Ienco, A.; Laschi, F.; Leoni, P.; Marchetti, F.; Marchetti, L.; Mealli, C.; Zanello, P. *J. Am. Chem. Soc.* **2005**, *127*, 3076.
- (17) Bokdam, M.; Cakir, D.; Brocks, G. *Appl. Phys. Lett.* **2011**, *98*, No. 113303.
- (18) García-Lastra, J. M.; Rostgaard, C.; Rubio, A.; Thygesen, K. S. *Phys. Rev. B* **2009**, *80*, No. 245427.
- (19) (a) Bergfeld, J. P.; Solomon, G. C.; Stafford, C. A.; Ratner, M. A. *Nano Lett.* **2011**, *11*, 2759. (b) Markussen, T.; Stadler, R.; Thygesen, K. S. *Nano Lett.* **2010**, *10*, 4260. (c) Nozaki, D.; Sevincli, H.; Avdoshenko, S. M.; Gutierrez, R.; Cuniberti, G. 2012, arXiv:1203.5269v1. arXiv.org e-Print archive. <http://arxiv.org/abs/1203.5269v1>. (d) Kaliginedi, V.; Moreno-García, P.; Valkenier, H.; Hong, W.; García-Suárez, V. M.; Buitter, P.; Otten, J. L. H.; Hummelen, J. C.; Lambert, C. J.; Wandlowski, T. *J. Am. Chem. Soc.* **2012**, *134*, 5262.
- (20) Guedon, C. M.; Valkenier, H.; Markussen, T.; Thygesen, K. S.; Hummelen, J. C.; van der Molen, S. *J. Nat. Nanotechnol.* **2012**, *7*, 305.
- (21) Satanin, A. M.; Hedin, E. R.; Joe, Y. S. *Phys. Lett. A* **2006**, *349*, 45.
- (22) (a) Finch, C. M.; García-Suárez, V. M.; Lambert, C. J. *Phys. Rev. B* **2009**, *79*, No. 033405. (b) Wei, Z.; Li, T.; Jennum, K.; Santella, M.; Bovet, N.; Hu, W.; Nielsen, M. B.; Bjørnholm, T.; Solomon, G. S.; Laursen, B. W.; Nørgaard, K. *Langmuir* **2012**, *28*, 4016.
- (23) (a) Park, H.; Park, J.; Lim, A. K. L.; Anderson, E. H.; Alivisatos, A. P.; McEuen, P. L. *Nature* **2000**, *407*, 57. (b) Zhang, J.; Kuznetsov, A. M.; Medvedev, I. G.; Chi, Q.; Albrecht, T.; Jensen, P. S.; Ulstrup, J. *Chem. Rev.* **2008**, *108*, 2737. (c) Leary, E.; Higgins, S. J.; van Zalinge, H.; Haiss, W.; Nichols, R. J.; Nygaard, S.; Jeppesen, J. O.; Ulstrup, J. *J. Am. Chem. Soc.* **2008**, *130*, 12204. (d) Meded, V.; Bagrets, A.; Fink, K.; Chandrasekar, R.; Ruben, M.; Evers, F.; Bernard-Mantel, A.; Seldenthuis, J. S.; Beukman, A.; van der Zant, H. S. J. *Phys. Rev. B* **2011**, *83*, No. 245415.